J Shoulder Elbow Surg (2021) ■, 1–11

ELSEVIER

Journal of Shoulder and Elbow Surgery

www.elsevier.com/locate/ymse

Does the Walch type B shoulder have a transverse force couple imbalance? A volumetric analysis of segmented rotator cuff muscles in osteoarthritic shoulders

Antonio Arenas-Miquelez, MD[a], Victor K. Liu, MD[a], Joseph Cavanagh, MBBS[b], Petra L. Graham, PhD[c], Louis M. Ferreira, PhD[b,d,e], Desmond J. Bokor, MBBS, FRACS, FAOrthA[a], George S. Athwal, MD, FRCSC[b,e], Sumit Raniga, BSc, MSc(Hons), MBChB, FRACS, FAOrthA[a,*]

[a]*MQ Health Translational Shoulder Research Program, Faculty of Medicine & Health Sciences, Macquarie University, Sydney, NSW, Australia*
[b]*Roth|McFarlane Hand and Upper Limb Centre, St. Joseph's Health Care, London, ON, Canada*
[c]*Centre for Economic Impacts of Genomic Medicine (GenIMPACT), Macquarie Business School, Sydney, NSW, Australia*
[d]*Department of Mechanical & Materials Engineering, The University of Western Ontario, London, ON, Canada*
[e]*Department of Surgery, Schulich School of Medicine and Dentistry, The University of Western Ontario, London, ON, Canada*

Background: The etiology of the Walch type B shoulder remains unclear. We hypothesized that a scapulohumeral muscle imbalance, due to a disturbed transverse force couple (TFC) between the anterior and posterior rotator cuff muscles, may have a role in the pathogenesis of the type B morphology. The purpose of this study was to determine whether there is a TFC imbalance in the Walch type B shoulder using an imaging-based 3-dimensional (3D) volumetric and fatty infiltration assessment of segmented rotator cuff muscles.
Methods: Computed tomography images of 33 Walch type A and 60 Walch type B shoulders with the complete scapula and humerus including the distal humeral epicondyles were evaluated. The 3D volumes of the entire subscapularis, supraspinatus, and infraspinatus–teres minor (Infra-Tm) were manually segmented and analyzed. Additionally, anthropometric parameters including glenoid version, glenoid inclination, posterior humeral head subluxation, and humeral torsion were measured. The 3D muscle analysis was then compared with the anthropometric parameters using the Wilcoxon rank sum and Kruskal-Wallis tests.
Results: There were no significant differences ($P > .200$) in muscle volume ratios between the Infra-Tm and the subscapularis in Walch type A (0.93) and type B (0.96) shoulders. The fatty infiltration percentage ratio, however, was significantly greater in type B shoulders (0.94 vs. 0.75, $P < .001$). The Infra-Tm to subscapularis fatty infiltration percentage ratio was significantly larger in patients with >75% humeral head subluxation than in those with 60%-75% head subluxation (0.97 vs. 0.74, $P < .001$) and significantly larger in patients with >25° of retroversion than in those with <15° of retroversion (1.10 vs. 0.75, $P = .004$). The supraspinatus fatty infiltration percentage was significantly lower in Walch type B shoulders than type A shoulders ($P = .004$). Walch type A shoulders had mean humeral retrotorsion of 22° ± 10° whereas Walch type B shoulders had humeral retrotorsion of only 14° ± 9° relative to the epicondylar axis ($P < .001$).

This study was reviewed and approved by the Western University Health Science Research Ethics Board (file no. 105912).

*Reprint requests: Sumit Raniga, BSc, MSc(Hons), MBChB, FRACS, FAOrthA, MQ Health Translational Shoulder Research Program, Faculty of Medicine & Health Sciences, Macquarie University, Sydney, NSW, Australia.

E-mail address: sumit.raniga@mqhealth.org.au (S. Raniga).

https://doi.org/10.1016/j.jse.2021.02.005

Conclusion: The TFC is in balance in the Walch type B shoulder in terms of 3D volumetric rotator cuff muscle analysis; however, the posterior rotator cuff does demonstrate increased fatty infiltration. Posterior humeral head subluxation and glenoid retroversion, which are pathognomonic of the Walch type B shoulder, may lead to a disturbance in the length-tension relationship of the posterior rotator cuff, causing fatty infiltration.

Level of evidence: Anatomy Study; Imaging

Keywords: Shoulder osteoarthritis; transverse force couple; rotator cuff; muscle volume; fatty infiltration; humeral torsion; CT images

In his 1974 and 1988 seminal publications, Professor Neer stated that there is frequent posterior erosion of the glenoid and posterior subluxation of the humeral head in primary glenohumeral joint osteoarthritis.[23,24] Friedman et al,[10] then Mullaji et al,[22] reported excessive retroversion of the glenoid in these patients. In their landmark publication, Walch et al[29] defined the type B glenoid. The Walch classification was further modified using 3-dimensional (3D) imaging in 2016.[2] The Walch type B shoulder has glenoid retroversion, posterior humeral head subluxation, and posteroinferior glenoid erosion.[2,6,7,29] A recent study has shown that the Walch type B humerus has significantly less retrotorsion than non-osteoarthritic shoulders.[27] Although our understanding of the bone deformity and its evolution in type B shoulders has improved, its etiology remains unclear.[6,7]

In 2014, Piepers et al[26] found no significant differences in the muscle volumes between the anterior (subscapularis) and posterior (infraspinatus and teres minor) rotator cuff muscles in nonpathologic shoulders. This finding suggests that the muscle volumes are in balance, and as a consequence, owing to the correlation between muscle strength and muscle volume, the transverse force couple (TFC) of nonpathologic shoulders is in balance. There are 2 recent studies investigating the state of the TFC in primary glenohumeral osteoarthritis that have used 2-dimensional (2D) cross-sectional representative computed tomography (CT) slices.[1,9] To date, there is limited literature on the complete volumetric assessment of the TFC in osteoarthritic shoulders. As such, the primary aim of this investigation was to determine whether there is a TFC imbalance in the Walch type B shoulder using an imaging-based, manually segmented, 3D volumetric assessment and fatty infiltration assessment of the rotator cuff muscles. The secondary aim was to study the relationship between the anthropometric glenohumeral parameters and 3D volumetric and fatty infiltration assessment of the rotator cuff muscles. We hypothesized that a scapulohumeral muscle imbalance, owing to a disturbed TFC between the anterior and posterior rotator cuff muscles, may have an association with the Walch type B morphology.

Materials and methods

Study groups

Digital Imaging and Communications in Medicine (DICOM) data were extracted from CT scans of Walch type A shoulders (n = 33; 19 left and 14 right shoulders) and Walch type B shoulders (n = 60; 31 left and 29 right shoulders). In the Walch type A group, there were 20 women and 13 men with an average age of 70 years (range, 50-87 years). In the Walch type B group, there were 24 women and 36 men with an average age of 71 years (range, 39-95 years). In all patients, glenohumeral joint osteoarthritis was clinically and radiographically diagnosed and CT scanning was performed for preoperative planning. Patients with rotator cuff tears, previous fractures, hardware, or tumors were excluded.

Glenoid parameters and Walch classification

Glenoid parameters including glenoid version, glenoid inclination, and posterior humeral head subluxation were analyzed using Blueprint 3D Preoperative Planning Software (Wright Medical, Memphis, TN, USA). Additionally, the 2D critical shoulder angle was measured from the preoperative radiographs of each type A and B shoulder as described by Moor et al.[21] Three experienced shoulder surgeons (G.S.A., D.J.B., and S.R.) classified each shoulder as type A or B and further into subtype groups (A1, A2, B1, B2, and B3) according to the Walch classification.[2]

Bone and muscle segmentation

By use of Mimics medical imaging software (version 22.0; Materialise, Leuven, Belgium), the whole scapula and humerus including the distal humeral epicondyles of all osteoarthritic shoulders in both groups were segmented from the Digital Imaging and Communications in Medicine (DICOM) data using a predefined bone thresholding mode (range, 226-2165 Hounsfield units).[3,4]

The 3D volumes of the entire subscapularis, supraspinatus, and infraspinatus–teres minor (Infra-Tm) were then manually segmented per Piepers et al[26] with the following modifications: The muscle volume masks were calculated from contours of not only the transverse but also the sagittal and coronal slices of the CT scan data to build a complete 3D volumetric mask of each of the rotator cuff musculotendinous units.[5] The first volume mask

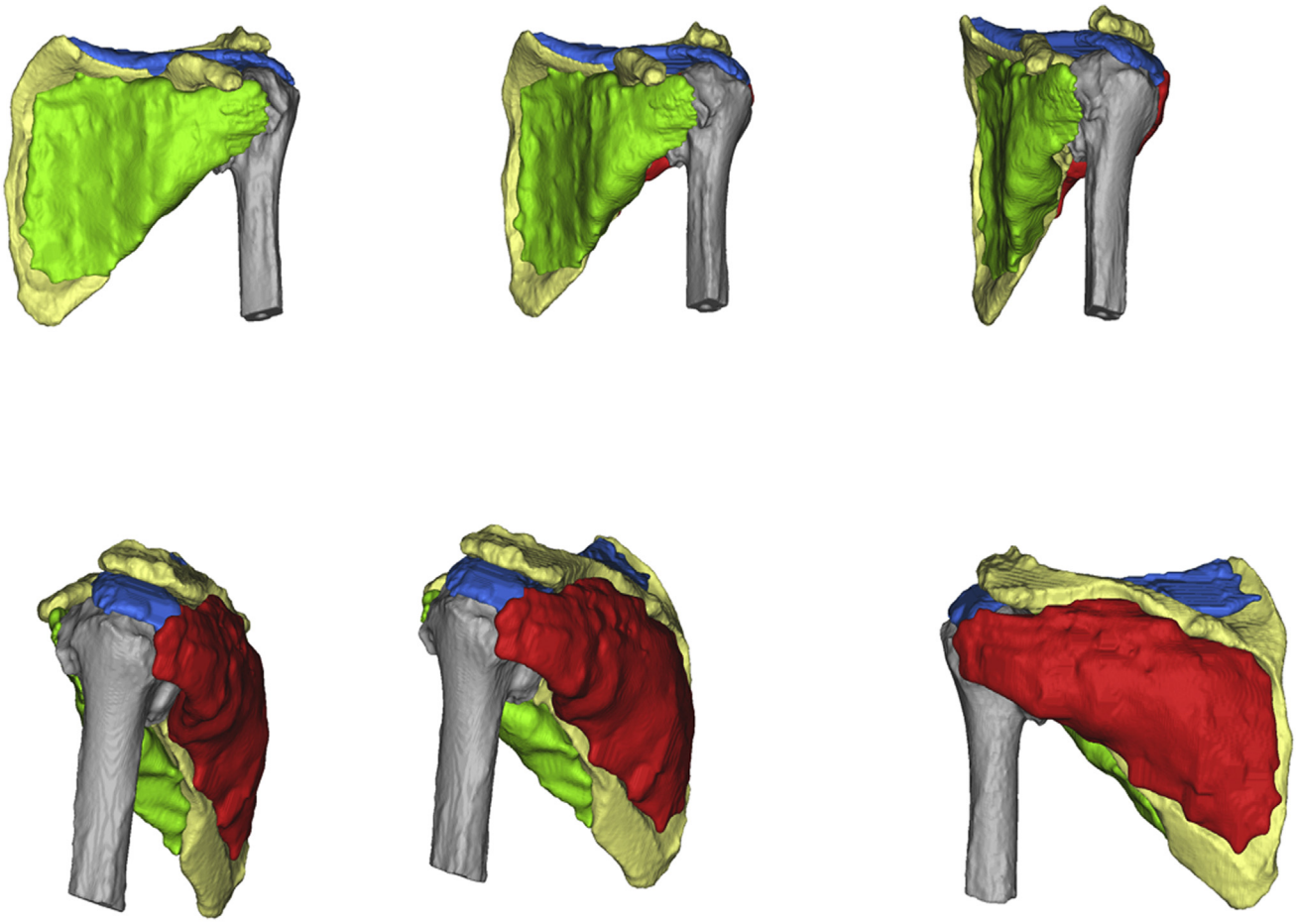

Figure 1 Reconstructions of manually segmented 3-dimensional volumetric assessment of supraspinatus (*blue*), infraspinatus (*red*), and subscapularis (*green*) musculotendinous units.

contained the subscapularis major and minor,[8] the second contained the Infra-Tm, and the third contained the supraspinatus (Fig. 1). The volumes of these masks, and therefore the defined muscle groups, were calculated using Mimics functions. The Infra-Tm to subscapularis volume ratio was also calculated.

To analyze fatty infiltration, a new mask was created by means of a predefined fat thresholding mode (−200 to −30 Hounsfield units) to calculate the fat volume within each of the rotator cuff muscle groups. The Infra-Tm to subscapularis fat volume ratio was also calculated. The 3D manual segmentation of the rotator cuff muscles was completed under the supervision of 2 fellowship-trained shoulder surgeons (A.A.-M. and S.R.) and a musculoskeletal radiologist.

Measurement of humeral head torsion with anatomic coordinate system

A previously published technique was used to calculate humeral head torsion.[25,27,31] An anatomic coordinate system was created to reference the intramedullary canal and the medial and lateral epicondyles for every humeral model. An anatomic humeral head–neck osteotomy plane was simulated, and its normal vector was projected down the long axis onto a plane containing the epicondylar axis (Fig. 2).[16,31] Humeral torsion was calculated as the angle (Θ) between the epicondylar axis and the normal osteotomy vector, using a custom MATLAB algorithm (The MathWorks, Natick, MA, USA). Measurements were repeated by 2 fellowship-trained shoulder surgeons (A.A.-M. and S.R.) to determine inter-rater reliability.

Statistical analysis

Two-way random-effects intraclass correlation coefficients were used to assess the inter-rater reliability (agreement) of muscle volume and humeral torsion calculation. Wilcoxon rank sum (WRS) tests were used to compare glenoid parameters and 3D volumetric measures between Walch type A and B shoulders. Kruskal-Wallis (KW) 1-way analysis of variance (ANOVA) was used to test for a difference in at least 1 pair of 3D volumetric measures between any of the glenoid subtypes. KW 1-way ANOVA was also used to determine whether there was a difference in 3D volumetric measures between categorical versions of the glenoid parameters: humeral torsion, head subluxation, and glenoid version. Head subluxation was split into 3 groups: 40% to <60%, 60%-75%, and >75% to 100%. Humeral torsion and retroversion were also split into 3 groups: <15°, 15°-25°, and >25°. This was done to better identify nonlinear relationships. If the KW P value was significant ($P < .05$), post hoc pair-wise WRS

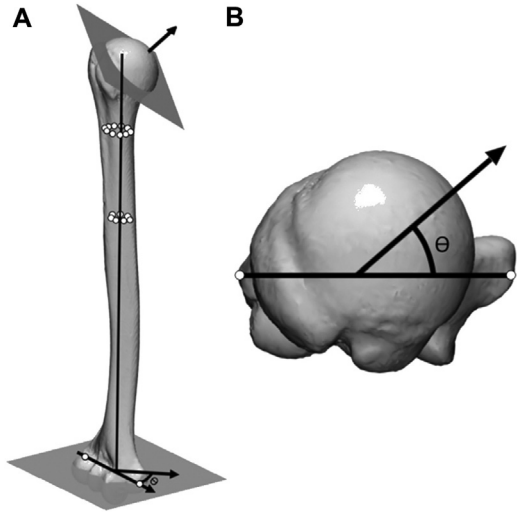

Figure 2 An anatomic coordinate system referencing the medial and lateral epicondyles was created for both the type A and type B groups. **(A)** Two sets of reference points were selected within the intramedullary canal at 20% and 40% of the humeral length, and their centers defined the long axis. A simulated humeral head osteotomy plane at the anatomic head-neck junction was created, and its normal vector was projected down the long axis onto a plane containing the epicondylar axis. Humeral torsion was defined as the angle *(Θ)* between the epicondylar axis and the normal osteotomy vector. **(B)** Axial view of normal vector of humeral head osteotomy plane and epicondylar axis, defined by medial and lateral epicondyles.

tests with P values adjusted for multiple comparisons using the Holm method were used to find which pairs of tests differed significantly.

Nonparametric methods were used because of the high likelihood that glenoid parameters and volumetric measures would not have been normally distributed. A significance level of 5% was used throughout. R statistical software (version 3.6.2; R Foundation for Statistical Computing, Vienna, Austria) was used for all analyses.

Results

Inter-rater reliability

For all parameters examined, excellent agreement was observed between the 2 fellowship-trained shoulder surgeons (Table I).

Anthropometric parameters

Walch type B shoulders had greater glenoid retroversion than Walch type A shoulders (22.0° ± 7.5° vs. 10.7° ± 4.8°, $P < .001$) and a greater humeral head subluxation percentage (80% ± 9% vs. 65% ± 12%, $P < .001$). Furthermore, Walch type B shoulders had significantly less humeral retrotorsion (14.5° ± 9.1°) than Walch type A shoulders (22.0° ± 9.5°) relative to the epicondylar axis ($P < .001$) (Fig. 3). There was no evidence of a difference in humeral torsion between male and female patients for either Walch type A ($P = .518$) or Walch type B ($P = .395$) shoulders or among female patients between Walch type A and B shoulders ($P = .100$). Among male patients, Walch type B shoulders had significantly less humeral retrotorsion (13.7° ± 9.0°) than Walch type A shoulders (23.4° ± 8.7°, $P = .005$).

Table I ICCs for agreement and 95% CIs

	ICC (95% CI)
Anthropometric glenohumeral parameters	
Humeral torsion	0.93 (0.92-0.97)
Segmented 3D muscle volumes	
Supraspinatus	0.96 (0.90-0.98)
Subscapularis	0.94 (0.86-0.98)
Infraspinatus–teres minor	0.98 (0.95-0.99)

ICC, intraclass correlation coefficient; *CI*, confidence interval; *3D*, 3-dimensional.

Three-dimensional volumetric assessment of rotator cuff muscles

The results of the 3D volumetric assessment of the manually segmented rotator cuff muscles and associated fatty infiltration percentages are shown in Tables II and III, respectively. The median segmented 3D volume of the entire Infra-Tm was significantly larger in Walch type B shoulders than in type A shoulders ($P = .026$, Table II). There were no statistically significant differences in subscapularis median segmented 3D volumes or fatty infiltration percentage between Walch type A and type B shoulders ($P > .08$, Table II) or among the various glenoid subtypes ($P > .16$, Table III). The mean Infra-Tm segmented 3D volume as a ratio of the subscapularis segmented 3D volume was 0.93 in type A and 0.96 in type B shoulders; this ratio was not significantly different between types ($P = .200$, Table II) or glenoid subtypes ($P = .202$, Table III). However, the Infra-Tm to subscapularis ratio for the fatty infiltration percentage was significantly larger in type B shoulders than type A shoulders (0.94 vs. 0.75, $P = .001$) and, similarly, for glenoid subtypes (0.82 for A1, 0.76 for A2, 1.31 for B2, and 0.97 for B3; $P = .005$, KW), with B2 and B3 significantly larger than A1 ($P = .012$ and $P = .021$, respectively, from WRS tests).

There were no statistically significant differences in median segmented 3D supraspinatus volumes between Walch type A and type B shoulders ($P = .192$) or among the various glenoid subtypes ($P = .239$). However, the

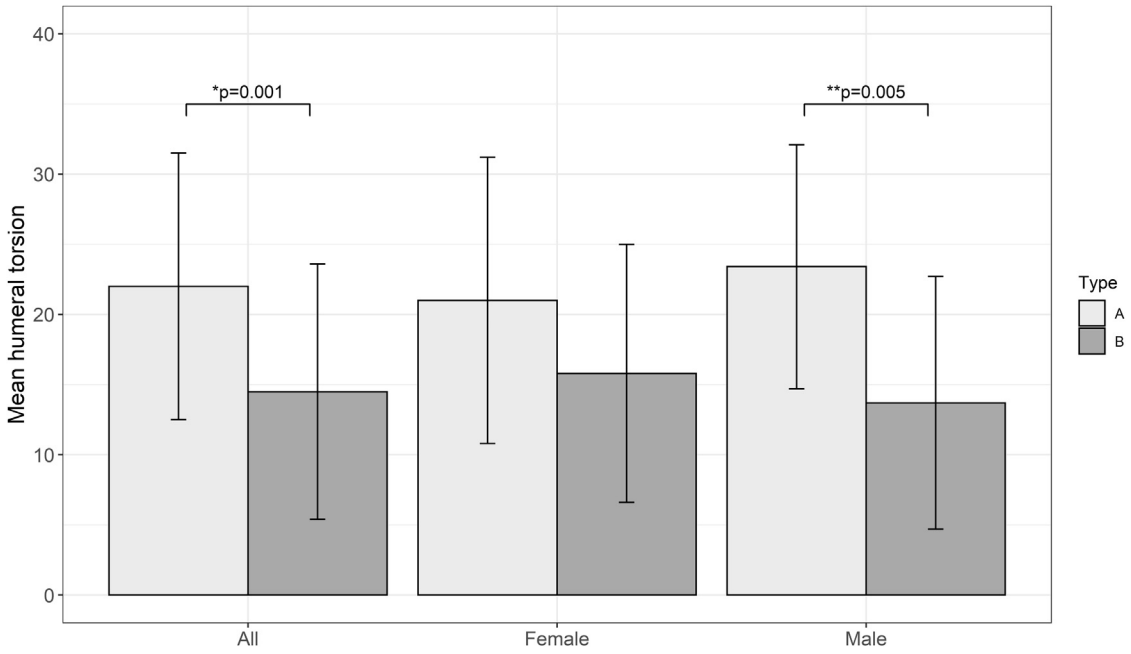

Figure 3 Mean humeral torsion for Walch type A and B shoulders across all patients and by sex with *error bars* representing ±1 standard deviation. Walch type A shoulders had significantly greater retrotorsion than type B shoulders across all patients (*$P = .001$) and for male patients (**$P = .005$).

Table II Median rotator cuff muscle volume and fatty infiltration percentage

Rotator cuff muscle	Median volume (IQR), cm^3			Median fatty infiltration % (IQR)		
	Walch type A	Walch type B	*P* value	Walch type A	Walch type B	*P* value
Supraspinatus	34.9 (23.2)	39.0 (24.5)	.192	8.1 (5.9)	4.5 (5.4)	.004*
SSC	126.4 (72.5)	145.3 (67.9)	.089	8.5 (4.9)	7.4 (4.2)	.273
Infra-Tm	110.0 (59.4)	134.7 (71.9)	.026*	6.6 (4.2)	6.6 (3.5)	.923
Infra-Tm/SSC ratio	0.93 (0.14)	0.96 (0.20)	.200	0.75 (0.23)	0.94 (0.40)	.001*

IQR, interquartile range; *SSC*, subscapularis; *Infra-Tm*, infraspinatus–teres minor.
P values were calculated with the Wilcoxon rank sum test.
* Statistically significant ($P < .05$).

Table III Difference between glenoid subtypes in median rotator cuff muscle volume and fatty infiltration percentage with IQR

Rotator cuff muscle	Median volume (IQR), cm^3					Median fatty infiltration % (IQR)				
	Glenoid subtype A1 (n = 26)	Glenoid subtype A2 (n = 7)	Glenoid subtype B2 (n = 42)	Glenoid subtype B3 (n = 18)	*P* value	Glenoid subtype A1 (n = 26)	Glenoid subtype A2 (n = 7)	Glenoid subtype B2 (n = 42)	Glenoid subtype B3 (n = 18)	*P* value
Supraspinatus	36.5 (20.9)	24.5 (6.5)	41.5 (25.8)	37.7 (17.5)	.239	6.4 (5.3)	13.1 (5.7)	4.3 (2.9)	6.8 (7.5)	.001*
SSC	134.2 (73.2)	85.8 (13.6)	149.3 (83.3)	144.3 (48.8)	.162	8.1 (5.4)	10.1 (4.2)	7.4 (4.1)	7.4 (4.2)	.223
Infra-Tm	118.0 (56.0)	80.8 (28.0)	138.3 (81.0)	124.7 (45.2)	.105	6.1 (3.7)	7.8 (3.9)	6.1 (3.2)	7.3 (2.7)	.120
Infra-Tm/SSC ratio	0.93 (0.12)	0.99 (0.14)	0.98 (0.20)	0.93 (0.17)	.202	0.82 (0.57)	0.76 (0.29)	1.31 (1.14)	0.97 (0.39)	.005*

IQR, interquartile range; *Infra-Tm*, infraspinatus–teres minor; *SSC*, subscapularis.
P values were calculated by Kruskal-Wallis 1-way analysis of variance.
* Statistically significant ($P < .05$).

Table IV Median (IQR) rotator cuff muscle volume and fatty infiltration percentage

Rotator cuff muscle	Median volume (IQR), cm^3	*P* value for median volume	Fatty infiltration % (IQR)	*P* value for fatty infiltration %
Head subluxation				
Supraspinatus	40% to <60%: 31.0 (18.3) 60%-75%: 42.7 (15.3) >75% to 100%: 36.1 (23.2)	.140	40% to <60%: 8.4 (6.2) 60%-75%: 4.1 (3.9) >75% to 100%: 5.5 (7.0)	.007*
Subscapularis	40% to <60%: 101.9 (43.4) 60%-75%: 153.9 (40.0) >75% to 100%: 121.6 (83.7)	.060	40% to <60%: 10.1 (3.9) 60%-75%: 7.3 (3.9) >75% to 100%: 7.6 (3.9)	.214
Infra-Tm	40% to <60%: 92.7 (28.7) 60%-75%: 144.4 (52.1) >75% to 100%: 118.2 (71.8)	.011*	40% to <60%: 6.9 (3.4) 60%-75%: 5.7 (3.0) >75% to 100%: 6.9 (3.0)	.072
Infra-Tm/SSC ratio	40% to <60%: 0.91 (0.13) 60%-75%: 0.95 (0.12) >75% to 100%: 0.98 (0.20)	.151	40% to <60%: 0.79 (0.39) 60%-75%: 0.74 (0.14) >75% to 100%: 0.97 (0.42)	<.001*
Humeral torsion				
Supraspinatus	<15°: 38.8 (23.9) 15°-25°: 41.07 (28.3) >25°: 29.1 (23.2)	.063	<15°: 4.4 (3.4) 15°-25°: 6.0 (7.8) >25°: 6.3 (8.2)	.186
Subscapularis	<15°: 143.3 (69.5) 15°-25°: 136 (72.5) >25°: 116.3 (78.6)	.414	<15°: 6.6 (4.0) 15°-25°: 7.2 (5.7) >25°: 8.5 (4.6)	.258
Infra-Tm	<15°: 123.6 (61.7) 15°-25°: 133.2 (83.4) >25°: 100.8 (61.0)	.199	<15°: 6.4 (3.4) 15°-25°: 6.8 (4.2) >25°: 6.5 (3.0)	.861
Infra-Tm/SSC ratio	<15°: 0.93 (0.22) 15°-25°: 0.96 (0.15) >25°: 0.91 (0.13)	.512	<15°: 0.94 (0.40) 15°-25°: 0.82 (0.34) >25°: 0.86 (0.24)	.172
Glenoid retroversion				
Supraspinatus	<15°: 36.5 (20.8) 15°-25°: 41.2 (24.5) >25°: 33.5 (21.9)	.168	<15°: 6.5 (6.6) 15°-25°: 3.9 (3.4) >25°: 5.5 (6.4)	.009*
Subscapularis	<15°: 122.9 (67.1) 15°-25°: 153.8 (66.8) >25°: 128.6 (65.2)	.140	<15°: 8.1 (4.6) 15°-25°: 6.6 (4.1) >25°: 8.1 (3.5)	.405
Infra-Tm	<15°: 114.6 (65.1) 15°-25°: 140.1 (71.4) >25°: 117.6 (55.9)	.163	<15°: 6.4 (3.9) 15°-25°: 5.8 (3.2) >25°: 7.7 (2.4)	.323
Infra-Tm/SSC ratio	<15°: 0.95 (0.13) 15°-25°: 0.94 (0.23) >25°: 0.95 (0.21)	.986	<15°: 0.75 (0.24) 15°-25°: 0.90 (0.50) >25°: 1.1 (0.37)	.004*

Infra-Tm, infraspinatus–teres minor; *SSC*, subscapularis.
P values were calculated by Kruskal-Wallis 1-way analysis of variance.
* Statistically significant ($P < .05$).

supraspinatus fatty infiltration percentage was significantly lower in Walch type B shoulders than in type A shoulders ($P = .004$). On comparison of glenoid subtypes (Table III), KW 1-way ANOVA indicated that the supraspinatus fatty infiltration percentage differed significantly between at least 1 pair of glenoid subtypes ($P = .001$). Pair-wise WRS tests showed that subtype A2 had significantly greater supraspinatus fatty infiltration than subtype B2 (13% vs. 4%, $P = .003$). Furthermore, the A2 subtype had greater supraspinatus fatty infiltration than subtype A1 glenoids, but it did not quite reach statistical significance (13.1% vs. 6.4%, $P = .052$).

Correlation between 3D volumetric assessment of rotator cuff muscles and anthropometric parameters

The degree of humeral head subluxation, humeral head torsion, and glenoid retroversion had no effect on muscle volumes with one exception (Table IV): The Infra-Tm volume differed between at least 1 pair of humeral head subluxation groups ($P = .011$, KW). Specifically, patients with subluxations of 60%-75% had 51.7 cm^3 more Infra-Tm volume than patients in the lower subluxation range of 40% to <60% (144.4 cm^3 vs. 92.7 cm^3; $P = .007$, WRS). The remaining pairs of subluxation groups were not significantly different ($P = .136$, WRS).

Fatty infiltration of the supraspinatus differed between at least 1 pair of humeral head subluxation degree groups ($P = .007$, KW) and glenoid retroversion groups ($P = .009$, KW) (Figs. 4 and 5, Table IV). Patients with 40% to <60% subluxation and those with ≥75% subluxation had significantly more supraspinatus fatty infiltration than those with head subluxation between 60% and 75% (8.4% vs. 4.1% [$P = .009$, WRS] and 5.5% vs. 4.1% [$P = .025$, WRS], respectively). Similarly, patients with <15° of glenoid retroversion had significantly greater supraspinatus fatty infiltration than those with glenoid retroversion between 15° and 25° (6.5% vs. 3.9%; $P = .010$, WRS). Furthermore, the Infra-Tm to subscapularis fatty infiltration percentage ratio differed significantly between head subluxation groups ($P < .001$, KW) and glenoid retroversion groups ($P = .004$, KW). The Infra-Tm to subscapularis fatty infiltration percentage ratio was significantly larger in patients with >75% to 100% head subluxation than in those with 60%-75% head subluxation (0.97 vs. 0.74; $P < .001$, WRS) (Fig. 4). Similarly, patients with >25° of glenoid retroversion had a significantly greater Infra-Tm to subscapularis fatty infiltration percentage ratio than those with <15° of retroversion (1.10 vs. 0.75; $P = .004$, WRS) (Fig. 5, Table IV).

Discussion

We hypothesized that an imbalanced TFC between the anterior and posterior rotator cuff muscle groups had an association in the pathogenesis of Walch type B morphology. The results of this clinical imaging–based investigation indicate that there was no statistically significant difference between Walch type A and type B shoulders in their ratio of posterior (Infra-Tm) to anterior (subscapularis) rotator cuff muscle volumes. As such, our primary hypothesis was rejected. However, the results did demonstrate a statistically significant difference in the Infra-Tm to subscapularis fatty infiltration ratio in Walch type B shoulders. Furthermore, the Infra-Tm to subscapularis fatty infiltration ratio correlated with the percentage of humeral head subluxation and the degree of glenoid retroversion. Although this fatty infiltration ratio within the Infra-Tm and subscapularis of type B shoulders did not correlate with humeral head retrotorsion, we found a statistically significant difference in humeral retrotorsion between the Walch type A and Walch type B humeri.

Walch et al[28] were the first investigators to publish the findings of static posterior subluxation of the humeral head before the development of posterior bony erosion or osteoarthritis. They described it as pre-osteoarthritic posterior subluxation of the humeral head, with humeral head subluxation preceding erosion. The etiology of this posterior humeral subluxation and the subsequent posteroinferior glenoid wear and its evolution remains unclear. Our understanding of the pathoanatomy of bone loss and its evolution in Walch type B glenoids has improved.[28] Knowles et al[17] demonstrated that patients with type B2 osteoarthritic glenoids have significantly greater premorbid paleoglenoid retroversion than patients with nonarthritic normal glenoids, suggesting that this premorbid morphologic variation may be one contributing factor to posterior glenoid erosion. Recently, Raniga et al[27] found that the Walch type B humerus has significantly less retrotorsion than non-osteoarthritic shoulders. They postulated that this may be an etiologic factor in posteroinferior glenoid wear and evolution or may simply be a compensatory manifestation of the arthritic process in the setting of a posteriorly subluxated humeral head. It has been theorized that the Walch type B3 glenoid may be a progression of the type B2 biconcave deformity.[30] Chan et al[6,7] compared glenoid parameters between type B2 and B3 shoulders with the hypothesis that the type B3 glenoid would have significantly worse retroversion, inclination, medialization, and posterior humeral head subluxation. Their results demonstrated no significant differences in the glenoid parameters between type B2 and B3 shoulders.[6,7] Raniga et al also found that there was no statistically significant difference in the humeral torsion or glenoid parameters between the type B2 and B3 shoulders.

Although we did not find any correlation between humeral torsion and any of the 3D volumetric rotator cuff parameters, including fatty infiltration, we did find a significant difference in humeral torsion between Walch type A and type B humeri. The Walch type A humeri had mean retrotorsion of 22°, whereas the Walch type B shoulders had humeral retrotorsion of 14°. Previous studies have found that non-osteoarthritic shoulders had approximately 36° of retrotorsion.[27,31] It is interesting to note that the Walch type A humerus does not have the same retrotorsion as the nonarthritic humerus but has greater retrotorsion than the type B humerus. Thus, there seems to be an association between altered humeral torsion and glenohumeral joint osteoarthritis, but it is not clear whether this difference in humeral torsion is a cause or an effect of the osteoarthritic process.

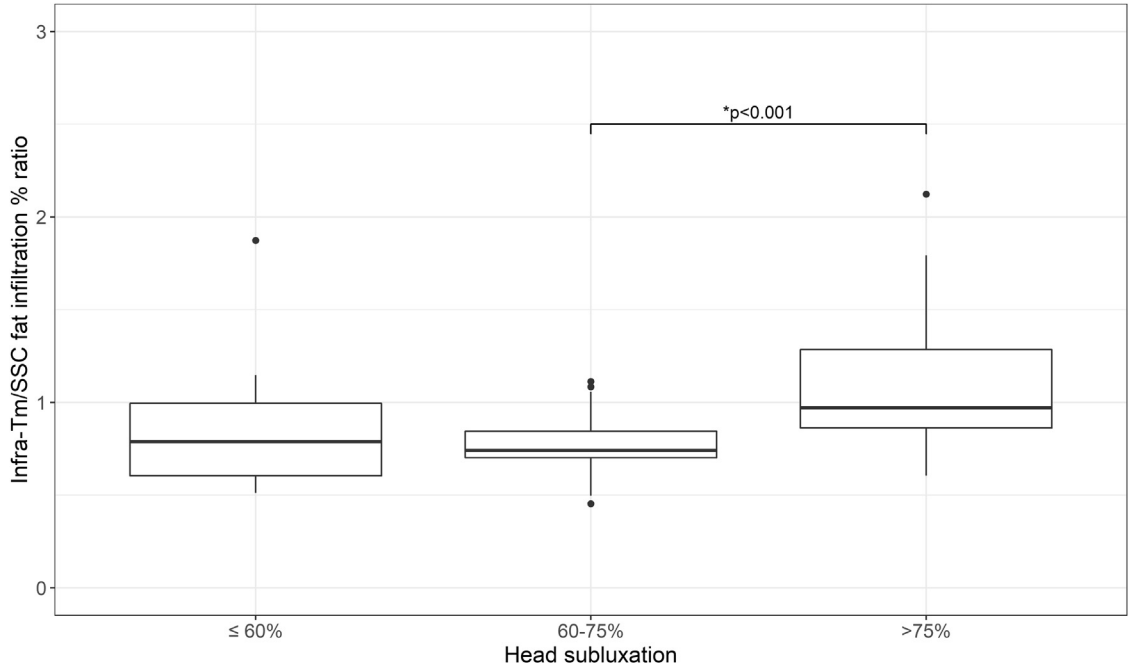

Figure 4 Box plot demonstrating infraspinatus–teres minor *(Infra-Tm)* to subscapularis *(SSC)* fatty infiltration percentage ratio in relation to defined groups of humeral head subluxation.

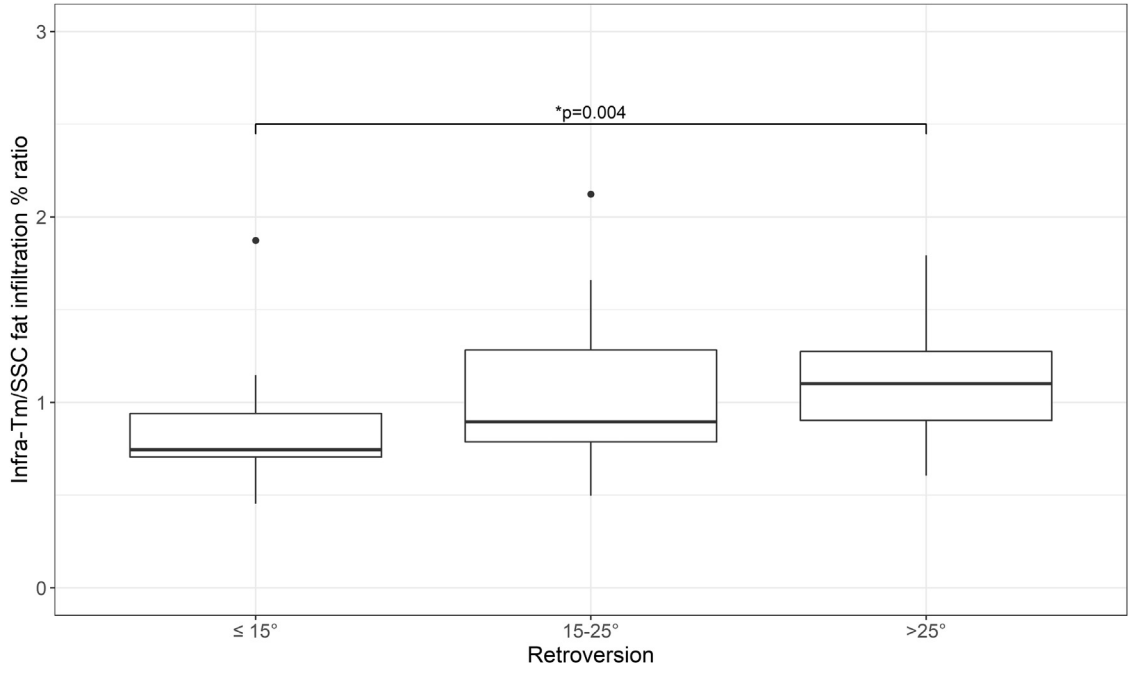

Figure 5 Box plot demonstrating infraspinatus–teres minor *(Infra-Tm)* to subscapularis *(SSC)* fatty infiltration percentage ratio in relation to defined groups of glenoid retroversion.

Overall, we believe the etiology of the Walch type B shoulder is multifactorial and it is likely related to a combination of bone and soft-tissue factors. Piepers et al[26] used an innovative CT-based technique to study the TFC in nonpathologic shoulders. They found no significant differences in the 3D manually segmented muscle volumes between the anterior and posterior rotator cuff, suggesting that the TFC of nonpathologic shoulders is in balance. Recently, Aleem et al[1] retrospectively measured rotator cuff muscle cross-sectional area on representative sagittal CT

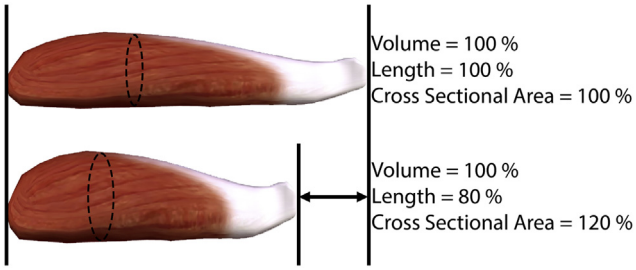

Figure 6 We hypothesize that posterior humeral head subluxation, with associated eccentric posterior wear and joint medialization, causes the length of the posterior rotator cuff to decrease. This results in an increased cross-sectional area in a 2-dimensional analysis of the muscle belly, with constant volume, per the Poisson effect. Hence, our 3-dimensional analysis of the entire volume demonstrated no difference.

slices of osteoarthritic shoulders. Using this 2D method to calculate the cross-sectional area, they found that there was a TFC imbalance in Walch type B shoulders with an increased posterior rotator cuff muscle area compared with the anterior rotator cuff muscle. The increased ratio of posterior-to-anterior rotator cuff 2D cross-sectional area was also associated with greater glenoid retroversion and humeral head subluxation. The authors postulated that there is a TFC muscle imbalance and the larger posterior rotator cuff musculature could promote a greater amount of posterior subluxation driving the type B evolution. We hypothesize that posterior humeral head subluxation, with associated eccentric posterior wear and joint medialization, causes the length of the posterior rotator cuff to decrease. This results in an increased cross-sectional area in a 2D analysis of the muscle belly, with a constant volume per the Poisson effect. Hence, our 3D analysis of the entire volume demonstrated no difference (Fig. 6).

Our study investigated the TFC in Walch type A and B shoulders using the same manually segmented 3D volumetric assessment as Piepers et al,[26] with the addition of supraspinatus muscle volume analysis. Although the use of cross-sectional areas on magnetic resonance imaging has been validated recently,[15] we believe that our methodology of quantifying the entire muscle volume allows for a more precise and reliable assessment of the rotator cuff. Furthermore, it allowed us to evaluate fatty infiltration as a percentage of the entire muscle volume. We correlated these 3D muscle volumes to the standard glenohumeral parameters (Walch glenoid subtype, glenoid version, inclination, and humeral head subluxation). However, we also studied the relationship of 3D muscle volumes to humeral head torsion. Contrary to Aleem et al,[1] we did not find a TFC imbalance with respect to the entire anterior and posterior muscle volumes, as discussed earlier. However, the Infra-Tm to subscapularis fatty infiltration ratio was increased, and this correlated with increasing glenoid retroversion and posterior humeral head subluxation. A high Infra-Tm to subscapularis fatty infiltration ratio means that the Infra-Tm has a greater percentage of fatty infiltration relative to the subscapularis. In contrast, a low ratio means that the Infra-Tm has a lower percentage of fatty infiltration relative to the subscapularis.

Fatty infiltration of the posterior rotator cuff musculature in glenohumeral osteoarthritis has been shown previously. Donohue et al[9] assessed rotator cuff muscle fatty infiltration by assigning the Goutallier score on the sagittal CT slice just medial to the spinoglenoid notch for each muscle in various osteoarthritic glenoid morphologies. They concluded that Walch type B deformity, with increased glenoid retroversion and increased joint-line medialization, was associated with predominantly posterior rotator cuff fatty infiltration. Furthermore, Walker et al[30] showed that patients with initial posterior humeral head subluxation and subsequent development of progression of posterior glenoid bone loss had a higher percentage of posterior cuff fatty infiltration as a percentage of cross-sectional muscle area.

In our study, the Infra-Tm to subscapularis fatty infiltration ratio was most significantly influenced by increasing humeral head subluxation and glenoid retroversion. Both of these anthropometric features are pathognomonic of the Walch type B shoulder. It is not clear whether the posterior rotator cuff fatty infiltration is a cause or a consequence of the Walch type B evolution. It has been shown that loss of tension in the rotator cuff musculotendinous unit leads to an increase in the pennation angle and reduction of sarcomeres in series with subsequent fatty infiltration between the fibrils.[11-14,18,20] The posterior humeral head subluxation, glenoid retroversion, joint medialization, and humeral head antetorsion in type B shoulders may lead to a disturbance in the length-tension relationship of the posterior rotator cuff, causing fatty infiltration. Therefore, we believe that fatty infiltration may be a consequence of the resulting disturbance. Although the TFC is in balance in the Walch type B shoulder with 3D volumetric analysis, the fatty infiltration of the posterior rotator cuff may cause a functional imbalance.

Furthermore, we found that there was an increased fatty infiltration percentage of the supraspinatus in Walch type A shoulders compared with type B shoulders. An interesting finding was that glenoid subtype analysis showed that the type A2 shoulders had the highest percentage of fatty infiltration of all the glenoid subtypes, twice as much as the type A1 shoulders. We believe that this is because of medialization that occurs in the A2 subtype, leading to loss of tension in the supraspinatus musculotendinous unit as described earlier.

This study has several limitations. We did not have a control group of non-osteoarthritic shoulders. The representative groups in the study were not equal in number. There were more male patients in the type B group as opposed to the type A group, which may have had an effect on the median segmented 3D volume. However, this would not affect any of the anterior to posterior rotator cuff ratio

calculations for volume or fatty infiltration percentage. Furthermore, we did not determine joint-line medialization in our analysis, which has been shown to be related to muscle fatty infiltration in previous studies.[9,30] Additionally, we used muscle volume as a surrogate for muscle force, which may not completely represent the muscle dynamics, including the line of pull and net load vector. Further investigations to understand the influence of the muscle line of pull and load vectors are necessary to fully comprehend the role of the rotator cuff in the evolution of the Walch type B shoulder.

There are several strengths in our study compared with prior investigations. First, we calculated 3D volumes of the entire musculotendinous unit instead of using the cross-sectional area on a single CT scan slice. Second, we quantified fatty infiltration in each musculotendinous unit instead of using the Goutallier classification on a representative sagittal slice.[19] Third, we included all the relevant anthropometric parameters, including humeral torsion, in our analysis.

Conclusion

The Walch type B shoulder is characterized by retroversion, bone loss, and humeral head subluxation. A TFC imbalance has been postulated to be an etiologic factor in posterior humeral head subluxation. Our results, assessing the 3D volumes of the anterior and posterior rotator cuff, demonstrated no significant differences in muscle volumes. However, the posterior rotator cuff was found to have increased fatty infiltration. On the basis of this study, posterior humeral head subluxation and glenoid retroversion, which are pathognomonic of the Walch type B shoulder, may lead to a disturbance in the length-tension relationship of the posterior rotator cuff, thus causing geographic fatty infiltration.

Acknowledgments

The authors acknowledge Nikolas K. Knowles and John Read.

Disclaimer

George S. Athwal is a consultant for Wright Medical Technologies. This company had no input into the design, methods, results, or preparation of this manuscript. All the other authors, their immediate families, and any research foundations with which they are affiliated have not received any financial payments or other benefits from any commercial entity related to the subject of this article.

References

1. Aleem AW, Chalmers PN, Bechtold D, Khan AZ, Tashjian RZ, Keener JD. Association between rotator cuff muscle size and glenoid deformity in primary glenohumeral osteoarthritis. J Bone Joint Surg Am 2019;101:1912-20. https://doi.org/10.2106/JBJS.19.00086
2. Bercik MJ, Kruse K II, Yalizis M, Gauci MO, Chaoui J, Walch G. A modification to the Walch classification of the glenoid in primary glenohumeral osteoarthritis using three-dimensional imaging. J Shoulder Elbow Surg 2016;25:1601-6. https://doi.org/10.1016/j.jse.2016.03.010
3. Bryce CD, Pennypacker JL, Kulkarni N, Paul EM, Hollenbeak CS, Mosher TJ, et al. Validation of three-dimensional models of in situ scapulae. J Shoulder Elbow Surg 2008;17:825-32. https://doi.org/10.1016/j.jse.2008.01.141
4. Budge MD, Lewis GS, Schaefer E, Coquia S, Flemming DJ, Armstrong AD. Comparison of standard two-dimensional and three-dimensional corrected glenoid version measurements. J Shoulder Elbow Surg 2011;20:577-83. https://doi.org/10.1016/j.jse.2010.11.003
5. Chalmers PN, Beck L, Stertz I, Aleem A, Keener JD, Henninger HB, et al. Do magnetic resonance imaging and computed tomography provide equivalent measures of rotator cuff muscle size in glenohumeral osteoarthritis? J Shoulder Elbow Surg 2018;27:1877-83. https://doi.org/10.1016/j.jse.2018.03.015
6. Chan K, Knowles NK, Chaoui J, Ferreira LM, Walch G, Athwal GS. Is the Walch B3 glenoid significantly worse than the B2? Shoulder Elbow 2018;10:256-61. https://doi.org/10.1177/1758573217724111
7. Chan K, Knowles NK, Chaoui J, Gauci MO, Ferreira LM, Walch G, et al. Characterization of the Walch B3 glenoid in primary osteoarthritis. J Shoulder Elbow Surg 2017;26:909-14. https://doi.org/10.1016/j.jse.2016.10.003
8. Collin P, Ladermann A, Le Bourg M, Walch G. Subscapularis minor—an analogue of the teres minor? Orthop Traumatol Surg Res 2013;99:S255-8. https://doi.org/10.1016/j.otsr.2013.03.003
9. Donohue KW, Ricchetti ET, Ho JC, Iannotti JP. The association between rotator cuff muscle fatty infiltration and glenoid morphology in glenohumeral osteoarthritis. J Bone Joint Surg Am 2018;100:381-7. https://doi.org/10.2106/JBJS.17.00232
10. Friedman RJ, Hawthorne KB, Genez BM. The use of computerized tomography in the measurement of glenoid version. J Bone Joint Surg Am 1992;74:1032-7.
11. Gerber C, Meyer DC, Fluck M, Benn MC, von Rechenberg B, Wieser K. Anabolic steroids reduce muscle degeneration associated with rotator cuff tendon release in sheep. Am J Sports Med 2015;43:2393-400. https://doi.org/10.1177/0363546515596411
12. Gerber C, Meyer DC, Frey E, von Rechenberg B, Hoppeler H, Frigg R, et al. Neer Award 2007: reversion of structural muscle changes caused by chronic rotator cuff tears using continuous musculotendinous traction. An experimental study in sheep. J Shoulder Elbow Surg 2009;18:163-71. https://doi.org/10.1016/j.jse.2008.09.003
13. Gerber C, Meyer DC, Schneeberger AG, Hoppeler H, von Rechenberg B. Effect of tendon release and delayed repair on the structure of the muscles of the rotator cuff: an experimental study in sheep. J Bone Joint Surg Am 2004;86-A:1973-82. https://doi.org/10.2106/00004623-200409000-00016
14. Goutallier D, Postel JM, Bernageau J, Lavau L, Voisin MC. Fatty muscle degeneration in cuff ruptures. Pre- and postoperative evaluation by CT scan. Clin Orthop Relat Res 1994:78-83.
15. Henninger HB, Christensen GV, Taylor CE, Kawakami J, Hillyard BS, Tashjian RZ, et al. The muscle cross-sectional area on MRI of the

shoulder can predict muscle volume: an MRI study in cadavers. Clin Orthop Relat Res 2020;478:871-83. https://doi.org/10.1097/CORR.0000000000001044

16. Knowles NK, Carroll MJ, Keener JD, Ferreira LM, Athwal GS. A comparison of normal and osteoarthritic humeral head size and morphology. J Shoulder Elbow Surg 2016;25:502-9. https://doi.org/10.1016/j.jse.2015.08.047
17. Knowles NK, Ferreira LM, Athwal GS. Premorbid retroversion is significantly greater in type B2 glenoids. J Shoulder Elbow Surg 2016;25:1064-8. https://doi.org/10.1016/j.jse.2015.11.002
18. Kuenzler MB, Nuss K, Karol A, Schar MO, Hottiger M, Raniga S, et al. Neer Award 2016: reduced muscle degeneration and decreased fatty infiltration after rotator cuff tear in a poly(ADP-ribose) polymerase 1 (PARP-1) knock-out mouse model. J Shoulder Elbow Surg 2017;26:733-44. https://doi.org/10.1016/j.jse.2016.11.009
19. Lee E, Choi JA, Oh JH, Ahn S, Hong SH, Chai JW, et al. Fatty degeneration of the rotator cuff muscles on pre- and postoperative CT arthrography (CTA): is the Goutallier grading system reliable? Skeletal Radiol 2013;42:1259-67. https://doi.org/10.1007/s00256-013-1660-1
20. Meyer DC, Hoppeler H, von Rechenberg B, Gerber C. A pathomechanical concept explains muscle loss and fatty muscular changes following surgical tendon release. J Orthop Res 2004;22:1004-7. https://doi.org/10.1016/j.orthres.2004.02.009
21. Moor BK, Bouaicha S, Rothenfluh DA, Sukthankar A, Gerber C. Is there an association between the individual anatomy of the scapula and the development of rotator cuff tears or osteoarthritis of the glenohumeral joint?: A radiological study of the critical shoulder angle. Bone Joint J 2013;95-B:935-41. https://doi.org/10.1302/0301-620X.95B7.31028
22. Mullaji AB, Beddow FH, Lamb GH. CT measurement of glenoid erosion in arthritis. J Bone Joint Surg Br 1994;76:384-8.
23. Neer CS II. Replacement arthroplasty for glenohumeral osteoarthritis. J Bone Joint Surg Am 1974;56:1-13.
24. Neer CS II, Morrison DS. Glenoid bone-grafting in total shoulder arthroplasty. J Bone Joint Surg Am 1988;70:1154-62.
25. Pearl ML, Volk AG. Retroversion of the proximal humerus in relationship to prosthetic replacement arthroplasty. J Shoulder Elbow Surg 1995;4:286-9.
26. Piepers I, Boudt P, Van Tongel A, De Wilde L. Evaluation of the muscle volumes of the transverse rotator cuff force couple in non-pathologic shoulders. J Shoulder Elbow Surg 2014;23:e158-62. https://doi.org/10.1016/j.jse.2013.09.027
27. Raniga S, Knowles NK, West E, Ferreira LM, Athwal GS. The Walch type B humerus: glenoid retroversion is associated with torsional differences in the humerus. J Shoulder Elbow Surg 2019;28:1801-8. https://doi.org/10.1016/j.jse.2019.1802.1010
28. Walch G, Ascani C, Boulahia A, Nove-Josserand L, Edwards TB. Static posterior subluxation of the humeral head: an unrecognized entity responsible for glenohumeral osteoarthritis in the young adult. J Shoulder Elbow Surg 2002;11:309-14. https://doi.org/10.1067/mse.2002.124547
29. Walch G, Badet R, Boulahia A, Khoury A. Morphologic study of the glenoid in primary glenohumeral osteoarthritis. J Arthroplasty 1999;14:756-60.
30. Walker KE, Simcock XC, Jun BJ, Iannotti JP, Ricchetti ET. Progression of glenoid morphology in glenohumeral osteoarthritis. J Bone Joint Surg Am 2018;100:49-56. https://doi.org/10.2106/JBJS.17.00064
31. West EA, Knowles NK, Athwal GS, Ferreira LM. A 3D comparison of humeral head retroversion by sex and measurement technique. Shoulder Elbow 2018;10:192-200. https://doi.org/10.1177/1758573217711897